THE JOURNAL OF BIOLOGICAL CHEMISTRY VOL. 286, NO. 40, pp. 34976–34985, October 7, 2011

Deregulation of microRNAs by HIV-1 Vpr Protein Leads to the Development of Neurocognitive Disorders*

Received for publication, March 21, 2011, and in revised form, August 2, 2011 Published, JBC Papers in Press, August 4, 2011, DOI 10.1074/jbc.M111.241547

Ruma Mukerjee[‡], J. Robert Chang[‡], Luis Del Valle[§], Asen Bagashev[‡], Monika M. Gayed[‡], Randolph B. Lyde[‡], Brian J. Hawkins[¶], Eugen Brailoiu[‖], Eric Cohen[**], Chris Power[‡‡], S. Ausim Azizi[‡], Benjamin B. Gelman[§§], and Bassel E. Sawaya[‡1]

*From the Departments of [‡]Neurology, and [‖]Pharmacology, Molecular Studies of Neurodegenerative Diseases Laboratory, Temple University School of Medicine, Philadelphia, Pennsylvania 19140, the [§]Department of Medicine, Section of Hematology/Oncology, and Department of Pathology, Stanley S. Scott Cancer Center, Louisiana State University School of Medicine, New Orleans, Louisiana 70112, [¶]Anesthesiology and Pain Medicine, Mitochondria and Metabolism Center, University of Washington, Seattle, Washington 98109, the **Institut de Recherches Cliniques de Montréal (IRCM) and Department of Microbiology and Immunology, Université de Montréal, Quebec, Canada, the [‡‡]Departments of Medicine (Neurology), Medical Microbiology & Immunology, and Psychiatry, University of Alberta, Edmonton, Alberta T6G 2S2, Canada, and the [§§]Departments of Pathology and Neuroscience & Cell Biology, Texas NeuroAIDS Research Center, University of Texas Medical Branch, Galveston, Texas 77555-0609*

Studies have shown that HIV-infected patients develop neurocognitive disorders characterized by neuronal dysfunction. The lack of productive infection of neurons by HIV suggests that viral and cellular proteins, with neurotoxic activities, released from HIV-1-infected target cells can cause this neuronal deregulation. The viral protein R (Vpr), a protein encoded by HIV-1, has been shown to alter the expression of various important cytokines and inflammatory proteins in infected and uninfected cells; however the mechanisms involved remain unclear. Using a human neuronal cell line, we found that Vpr can be taken up by neurons causing: (i) deregulation of calcium homeostasis, (ii) endoplasmic reticulum-calcium release, (iii) activation of the oxidative stress pathway, (iv) mitochondrial dysfunction and *v*-synaptic retraction. In search for the cellular factors involved, we performed microRNAs and gene array assays using human neurons (primary cultures or cell line, SH-SY5Y) that we treated with recombinant Vpr proteins. Interestingly, Vpr deregulates the levels of several microRNAs (*e.g.* miR-34a) and their target genes (*e.g.* CREB), which could lead to neuronal dysfunctions. Therefore, we conclude that Vpr plays a major role in neuronal dysfunction through deregulating microRNAs and their target genes, a phenomenon that could lead to the development of neurocognitive disorders.

Although effective in prolonging the life expectancy in patients with HIV infection (1), the highly active antiretroviral therapy (HAART)[2] in fact has resulted in an increased prevalence of HIV-associated neurocognitive disorders (HAND) (2). The molecular mechanisms leading to this phenomenon remain to be elucidated. Several reports indicated that HIV-infected macrophages and microglia produce neurotoxins (*e.g.* viral and cellular proteins) that have the ability to cause neuronal deregulation and to promote HAND (3, 4).

The viral protein R (Vpr) is among the released HIV-1 proteins that have been considered to be deleterious to neurons; however the molecular mechanisms involved remain unclear (5–7). Vpr is packaged into the virion, and is essential for HIV-1 replication in macrophages (8, 9). Infected brain cells have been shown to release Vpr that could affects neuronal growth (10). Vpr mediates multiple functions, including nuclear import of the HIV-1 pre-integration complex, G_2 cell cycle arrest, transactivation of both viral replication, and host genes and induction of apoptosis (11, 12). Vpr was also detected in a soluble form in CSF and sera of HIV-infected patients displaying neurological disorders (10). Vpr causes neuronal degeneration both *in vitro* and *in vivo* (7, 10, 13).

A calcium channel is an ion channel, which displays selective permeability to Ca^{2+} ions. It is sometimes synonymous as voltage-dependent Ca^{2+} channel (VDCC) (14). Activation of particular VDCCs allows Ca^{2+} entry into the cell, which depending on the cell type, results in muscular contraction, excitation of neurons, up-regulation of gene expression, or release of neurotransmitters. Five Ca^{2+} channels have been identified (L, P/Q, N, R, and T) (15). Neurons use both Ca^{2+} influx through plasmalemma Ca^{2+} channels and Ca^{2+} release from internal stores. Intracellular Ca^{2+} release channels are inositol 1,4,5-trisphosphate ($InsP_3$ orIP_3)-gated, referred to as IP_3 receptors (IP_3Rs) and Ca^{2+}-gated also known as ryanodine receptors (RyRs) (16). Cytosolic Ca^{2+} regulates IP3Rs and RyRs channels. We previously demonstrated the ability of Vpr to depolarize the neuronal membrane, to promote Ca^{2+} release through L- and P/Q-type channels and to induce Ca^{2+} release from internal stores such as the ER (data not shown). Perturbed Ca^{2+} homeostasis can mediate cell degeneration and eventually cell death by apoptosis (17). During normal signaling, IP_3Rs-mediated Ca^{2+} transients may be transmitted to the mitochondria, rais-

* This work was supported, in whole or in part, by National Institutes of Health Grant NINDS, R01-NS059327 (to B. E. S.). This work was also conducted with support from Harvard Catalyst, The Harvard Clinical and Translational Science Center (National Institutes of Health Award UL1 RR 025758 and financial contributions from Harvard University and its affiliated academic health care centers).

[1] To whom correspondence should be addressed: Molecular Studies of Neurodegenerative Diseases Lab, 3420 North Broad Street, MRB 719; Philadelphia, PA 19140. Tel.: 215-707-5446; Fax: 215-707-5948; E-mail: sawaya@temple.edu.

[2] The abbreviations used are: HAART, highly active anti-retroviral therapy; HAND, HIV-associated neurocognitive disorders; Vpr, viral protein R; VDCC, voltage-dependent Ca^{2+} channel; miRNA, microRNA; ISH, *in situ* hybridization.

ing mitochondrial matrix Ca^{2+} and enhancing mitochondrial bioenergetics. However, excess Ca^{2+} can lead to mitochondrial Ca^{2+} overload and mitochondrial dysfunction (18).

Note that mitochondria are distributed along the axon and control ATP levels and cell-to-cell communication (19). Regulation of mitochondrial distribution is particularly important in neurons, whose extended processes are highly dependent on organelle transport to balance the changing energy needs of each portion of the cell and any disturbance could lead to neurodegeneration (20).

microRNAs (miRNAs) have been defined as regulators of endogenous genes and their involvement in neurodegenerative diseases has been previously described (21–25). In HIV-1-infected cells, miRNAs have been shown to be conserved factors whose complete suppression is incompatible with cellular viability. HIV-1 can reshape the infected cells miRNAs expression profile. One interpretation of this latter finding is that the virus has learned to repress the expression of virus-targeted miRNAs, while enhancing the expression of propitious miRNAs that upregulate protein factors that benefit HIV-1 replication (26).

The limited information available regarding the neuropathogenic properties of HIV-1 Vpr and its *in vivo* effects gave us the rationale to examine whether Vpr contributes to the development of HAND and the mechanisms involved and whether these mechanisms required the implication of miRNAs and their target genes.

EXPERIMENTAL PROCEDURES

Cytosolic Ca^{2+} Concentrations—The human neuroblastoma cell line (SH-SY5Y) (13) were grown in DMEM + 10% FBS on coverslips (25 mm diameter). SH-SY5Y was chosen because of its ability to mirror pathways involved in neurodegenerative process associated with HIV-E. SH-SY5Y (5×10^5) were allowed to adhere and acclimate for 1 day prior to being treated with 10 mM of retinoic acid (RA) (Sigma) for 4 days to induce differentiation. For calcium measurement and mobilization, the cells were loaded with 5 μM fura-2 AM (Fura-2 AM is a fluorescent dye used to measure calcium concentrations inside the cells) (Invitrogen, Carlsbad, CA) for 45 min in the dark prior to Vpr treatment. Vpr protein was given at 10 pg/ml (equal to 10 nM). The coverslips were mounted on on the stage of an inverted microscope Nikon Eclipse TiE (Optical Apparatus Co., Ardmore, PA) as previously described (27). The ratio of the fluorescence signals (340/380 nm) was converted to Ca^{2+} concentrations.

Western Blot Analysis and Antibodies—Human neuronal SH-SY5Y cells (1×10^6) were treated with 10 pg/ml of Vpr protein for 24 h. Cells were then harvested and resuspended in lysis buffer as described by the manufacturer (Fermentas, MD). Western blotting (50 μg/sample) was performed on cell lysates 24 h post-transfection or treatment as described (28). Antibodies against SERP1, Drp-1, IRBIT, CREB, NEFM, Vpr, Cox IV, and Grb2 were used to detect the level of these proteins.

Immunohistochemistry—Frontal lobe brain tissue was banked by the Texas NeuroAIDS Research Center according to established protocols. Cases were classified and characterized according to the National NeuroAIDS Tissue Consortium guidelines. HIV-positive patients with varying degrees of dementia were selected, along with non-demented, HIV-negative controls. The formalin-fixed and paraffin-embedded tissues were sectioned at 5 μm thickness and placed on electromagnetically charged glass slides. Sections were deparaffinized in xylene and re-hydrated through descending grades of alcohol up to water. Immuno-histochemistry was performed utilizing an Avidin-Biotin-Peroxidase methodology, according to the manufacturer's instructions (Vectastain Elite ABC Peroxidase kit; Vector Laboratories Inc., Burlingame, CA). Non-enzymatic antigen retrieval was performed in citrate buffer for 30 min at 95 °C in a vacuum oven. After a 20 min cooling period, sections were rinsed with PBS and endogenous peroxidase was quenched with 3% H_2O_2 in methanol for 30 min. Sections were then rinsed with PBS, and a blocking step was performed with normal goat serum at room temperature in a humidified chamber for 2 h. Primary antibodies were incubated overnight at room temperature and included a rabbit polyclonal anti-Vpr (1:500 dilution, obtained through the AID Research Reagent Program, Division of AIDS, NIAID, NIH: Antiserum to Vpr 1–46, from Dr. Jeffrey Kopp). After rinsing with PBS, sections were incubated for 1 h at room temperature with biotinylated anti-rabbit secondary antibodies. The tissue was subsequently incubated with avidin-biotin-peroxidase complexes for 1 h at room temperature according to the manufacturer's instructions (Vector Laboratories), and finally, the sections were developed with a diaminobenzidine substrate (Sigma), counterstained with hematoxylin and coverslipped with Permount (Fisher Scientific).

Double Labeling Immunofluorescence—Cells in culture were fixed for 3 min in 3% buffered formalin, rinsed with PBS and blocked wit normal horse serum for 1 h. A mouse monoclonal anti MAP-2 antibody (1:100 dilution, Clone SMI-52, Covance, Berkeley, CA) was incubated for 2 h at room temperature, after which cells were incubated with a fluorescein-tagged anti-mouse antibody for 1 h. Cells were then blocked in normal goat serum and incubated with a rabbit polyclonal anti-CREB antibody (1:200 dilution, Cell Signaling) for hours. Finally cells were incubated with a rhodamine-tagged anti-rabbit secondary antibody, cover-slipped with an aqueous-based mounting media and visualized with an inverted fluorescent antibody equipped with deconvolution software (Slide Book 5, Intelligent Imaging).

miRNA Array Assay—Primary human neurons (HN) purchased from ScienCell Research Laboratories (Carlsbad, CA) and SH-SY5Y neuronal cells (5×10^5) were treated with Vpr (10 pg/ml) for 24 h. Total RNA was isolated using Trizol (Invitrogen). 750 ng of total RNA was used for miRNA array analysis using miRCURY LNA™ microRNA Array, v. 11.0 (Exiqon, Woburn, MA). In brief, RNA was labeled using the miRCURY LNA™ miRNA, Hy5 Power Labeling Kit (Exiqon) per manufacturer's recommendations using Maui SC Hybridization Chambers (BioMicro Systems, Salt Lake City, UT). Array chips were scanned using Axon GenePix Scanner (Molecular Devices, Downingtown, PA) and Genepix 4000 image capture software (Molecular Devices, Downingtown, PA). Quantile normalization was used using JMP Genomics (JMP, Cary, NC) and differentially regulated miRNA was determined. Untreated cells were used as control.

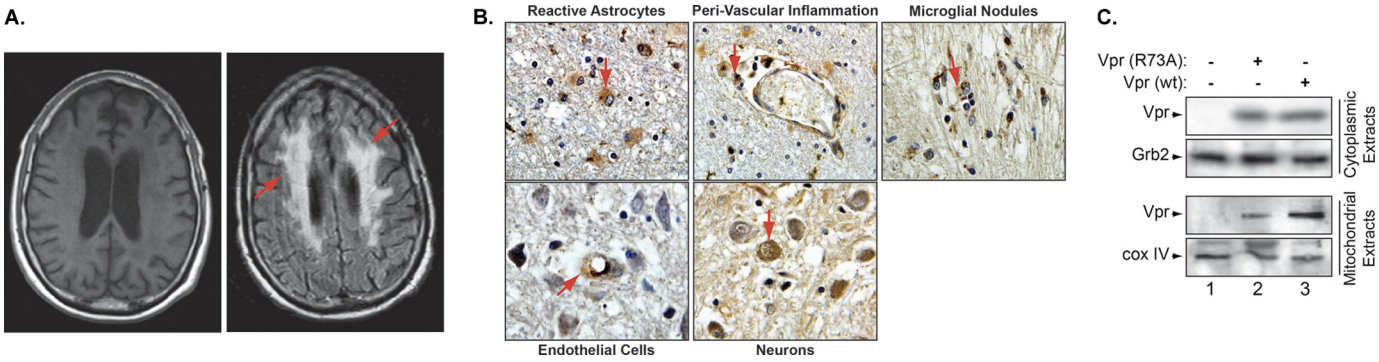

FIGURE 1. **Expression of Vpr in brain tissue of HIV-Encephalitis and in neuronal cells.** *A*, axial fluid attenuation inversion recovery (*FLAIR*) magnetic resonance images (*MRI*): without focal brain parenchymal signal abnormalities in a normal individual/patient (*left panel*) and demonstrating extensive, confluent increased T2 signal in the periventricular, subcortical, and deep white matter consistent with HIV leukoencephalopathy in patient with known HIV-1 infection (*right panel*). *B*, *arrows* depict the presence of Vpr in different cell types of the brain, including reactive astrocytes, perivascular lymphocytes, and giant multinucleate cells, activated microglial cells and endothelial cells. Neurons also express Vpr, preferentially neurons located right on the sites on inflammation. *C*, Western blot analysis of the presence of Vpr protein in 50 μg of cytoplasmic or mitochondrial extracts prepared from SH-SY5Y cells untreated or treated with Vpr proteins.

Genomic Gene Array and Data Analysis Methods—Gene expression profiling was performed using the Affymetrix GeneChip® HG-U133 set (Affymetrix, Santa Clara, CA), comprised of two microarrays that represent greater than 33,000 of the best-characterized human genes and almost a total of 45,000 probe sets. Labeling, hybridization and detection of RNA were done at the Genomics Core Facility at Thomas Jefferson and at HC-LITT-Harvard Universities according to recommendations by Affymetrix. Housekeeping control genes and spike controls were routinely analyzed on the GeneChip® microarrays to confirm the successful labeling of target RNAs. Preliminary data analysis was performed in conjunction with the Thomas Jefferson or Harvard Universities Bioinformatics Program. GeneChip® array results were also correlated with the array design and annotation information using the NetAffx™ Analysis Center. Hierarchical cluster analysis and heat maps were generated using Spotfire DecisionSite 7.2.

Validation of miRNAs by qPCR—miRNAs validation was performed using Illumina qPCR machine and RNA extracted from primary fetal neurons or human cell line as described above. First, miRNA cDNA synthesis was performed using Universal cDNA Synthesis Kit (Exiqon) followed by real-time PCR for miR-1, -7, -34a, and -96 using SYBR Green Master Mix, Universal RT using miRNA-specific microRNA LNA™ PCR primer sets (Exiqon).

Validation of miRNA Target Gene Expressions—Real-time PCR was performed using the following primers (purchased from IDT): 5′-GCCGCGAAGATGGTCGCCAA and 5′-TCGGGGGCATTTCTCGAG GTCT as forward and reverse primers for SERP1; 5′-TGGCGCAAGCTCTACTTG and 5′-GGCACTGA AGGCGATGAG as forward and reverse primers for Orai; 5′-GTTCTCAGGTGGACCATGTC and 5′-AGT TCTATCAGTGCCAAAGCC as forward and reverse primers for IRBIT; 5′-ACTTGACCTCCCTACTGGC and 5′-TCCTCTATCCCGTTGACACC as forward and reverse primers for Drp-1; 5′-AAGTGGGAAATGGCTCGTC and 5′-TCTAGTCTCTTCACC CTCCAG as forward and reverse primers for NEFM; 5′-GGCAGACAGTTCAAGTCCA TG and 5′-CGCTTTTGGGAATCAGTTACAC as forward and reverse primers for CREB; 5′-TTGTGTCTCCCTTG TCCATG and 5′-GGTCAAATCCCTCT GAGATCC as forward and reverse primers for STIM1; and 5′-CAGTGTCATGGTTCCTTTGC and 5′-GTTTCATG ATAGCAAGCGGTTC as forward and reverse primers for SIRT1. Amplifications were performed on Mastercycler ep realplex Thermocycler (Eppendorf, Hauppauge, NY) using FastStart Universal SYBR Green Master (Roche Diagnostics, Indianapolis, IN). PCR conditions for the amplifications were 95 °C for 5 min followed by 45 cycles of 95 °C for 30 s and 60 °C for 1 min. GAPDH was used as normalizing control using 5′-GCCTTCCGTGTTCCTACC and 5′-CCTC AGTGTAGCCCAAGATG as forward and reverse primers.

Brain Tissues Prepared from Vpr-transgenic Mice—Vpr transgenic mice were described previously, in which vpr was under the control of the c-fms (M-CSF receptor) promoter, permitting expression mainly in monocytoid cells (7, 29).

In Situ Hybridization (ISH)—miRCURY LNA™ microRNA Detection (FFPE), Optimization Kit 4 (miR-124) and has-miR-34a detection probe (3′-amino labeled) were purchased from Exiqon. The experiment was performed as suggested by the manufacturer using mice brain tissue (parental and Vpr-transgenic).

Statistics—Statistical analyses were used in all the experiments using Student's *t* tests, or unbalanced ANOVA analysis. Further, each experiment was repeated 3 times where 5 different cell fields were analyzed (each contains 10 cells). The results were considered statistically significant if $p < 0.01$.

RESULTS

Detection of Vpr in Neural Cells in Vivo—Radiologically, progressive HIV-1 dementia is characterized by cerebral atrophy with diffuse white matter hyper-intensity signal change that could be observed in the bilateral peri-ventricular frontal and parieto-occipital regions as displayed in Fig. 1*A* (*right panel*) when compared with the normal control (*left panel*). Therefore, we sought to determine the factors leading to this brain deterioration by studying the role of HIV-1 Vpr protein and its possible involvement in such development. First, we examined the presence of Vpr in neurons *in vivo* using human brain tissues derived from AIDS patients with HIV-encephalitis. As shown in Fig. 1*B*, using Vpr specific antibodies, immuno-histochemi-

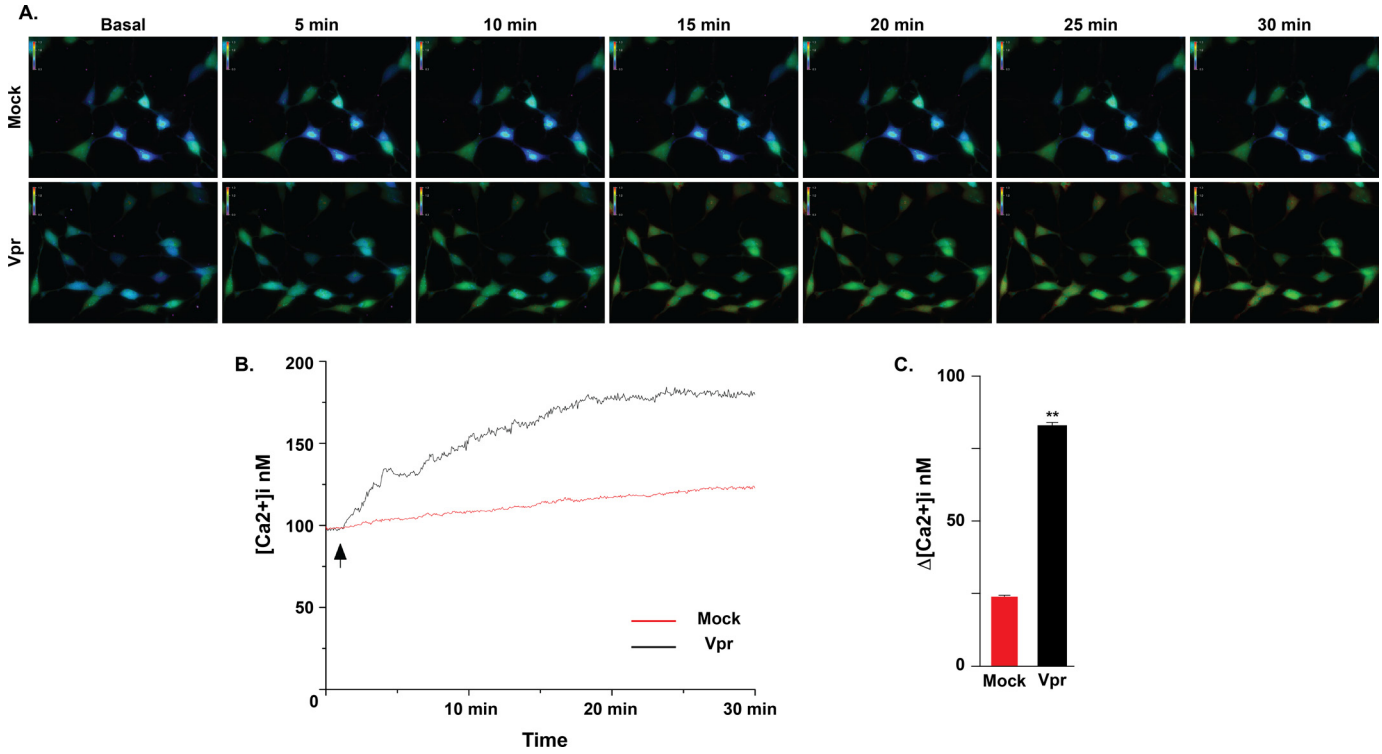

FIGURE 2. **Vpr increases calcium concentration.** *A*, SH-SY5Y cells were incubated with Fluo-2 AM and intracellular calcium was measured every 3 s using an inverted microscope Nikon Eclipse TiE (Optical Apparatus Co., Ardmore, PA) as previously described (27). The ratio of the fluorescence signals (340/380 nm) was converted to Ca^{2+} concentrations. The figure represents a montage of images collected from cells at T = 0 s and T = 5, 10, 15, 20, 25, and 30 min. Note that the calcium level varies between *blue* (basal), *green*, *yellow*, and *red* (highest increase). *B*, histogram showing calcium traces measurement in these cells. The experiment was repeated three times with similar results. *C*, all measurements were performed using n ≈ 50, and the results are statistically significant using Student's *t* test ($p < 0.05$). ($\Delta[Ca^{2+}]_i$ nM means the difference between basal Ca^{2+} and the maximal effect.)

cal experiments demonstrate the presence of Vpr in the cytoplasm of reactive astrocytes in sub-cortical regions of the brain, in close proximity to areas of inflammation. Vpr is also robustly expressed in perivascular cuffs of inflammatory cells, including multi-nucleated giant cells, and in parenchymal microglial nodules. Endothelial cells show intense immuno-reactivity for Vpr in sites of inflammation. Neurons adjacent to areas of microglial nodules and encephalitis showed expression of Vpr in agreement with the data reported earlier (7, 30).

Uptake and Detection of Vpr in Neurons—Next, we sought to confirm the presence and subcellular localization of Vpr in human brain cells *in vitro*. Neuronal cell line, SH-SY5Y cells were treated with 10 pg/ml of recombinant Vpr protein. Vpr protein was generated using baculovirus expression system (7). Twelve hours after Vpr treatment, the cells were thoroughly washed to remove any traces of Vpr and then lysed. Cell extracts were prepared and analyzed by Western blot using anti-Vpr antibody. As shown in Fig. 1*C*, Vpr protein was detected in cytoplasmic and mitochondrial extracts. To ascertain equal protein loading, anti-Grb2 or Cox IV antibodies were used. Hence, diverse cells including SH-SY5Y can take up Vpr (31). Note that the absence of Vpr in nuclear extracts should be further examined using additional time points.

Vpr Induces Ca^{2+} Accumulation Inside the Cells—Next, we examined the ability of Vpr to increase Ca^{2+} mobilization. SH-SY5Y cells (1×10^5) grown in serum-free media were treated with 10 pg/ml of Vpr protein. The cells were incubated with Fluo-2 AM and intracellular calcium was measured. As shown in Fig. 2*A*, exposure of the cells to Vpr elevates $[Ca^{2+}]_i$ inside the cells as early as 30 s. This level keeps increasing even at $t = 30$ min when compared with the Mock untreated cells as also shown in *panel B*. Note that the calcium level varies between blue (basal), green, yellow, and red (highest increase).

The average cytosolic Ca^{2+} concentration $[Ca^{2+}]_i$ was 83 ± 0.9 nM ($n = 47$) in Vpr-treated cells and 24 ± 0.5 ($n = 41$) in untreated cells (Panel C). ($\Delta[Ca^{2+}]_i$ nM means the difference between basal Ca^{2+} and max effect). Interestingly, Ca^{2+} mobilization increases simultaneously in the neurites and in the cell body in Vpr-treated cells (*panel A*).

Identification of miRNAs Regulated by Vpr in SH-SY5Y Cells—Involvement of miRNAs in other neuronal degenerative diseases and the ability of Vpr to be taken up by neurons, prompted us to examine the status of miRNAs and their target genes in Vpr-treated neurons. Neuronal cell line, SH-SY5Y, was treated with 10 pg/ml of Vpr protein for 24 h after which, total RNA was isolated and processed for miRNAs array assay. As shown in Fig. 3*A*, several miRNAs were differentially expressed (positively or negatively) in the presence of Vpr protein, suggesting that Vpr affects miRNAs levels in these cells. Similar results were obtained with primary human cultures of neurons (HN) (data not shown).

The levels of the most up-regulated miRNAs were then validated by qPCR in SH-SY5Y cells treated with Vpr wild type or its mutant (R73A). As shown in *panel B*, up-regulation of these miRNAs was at least 10-fold in Vpr- (yellow) but not in R73A-treated cells (purple) compared with the control (blue).

Because Vpr is not the only HIV-released viral proteins, we performed miRNA array using RNA isolated from SH-SY5Y cells treated with either Tat or gp120 proteins (HIV-1_{JR-FL}) or with supernatant collected from HIV-1_{JR-FL}-infected U937 cells. miRs-1, -7, -34a, and -96 were among the most up-regulated miRNAs as confirmed by qPCR (*panel C*, overlapped area).

Identification and Validation of Genes Regulated by Vpr in Neurons—Because miRNA regulates mRNA levels of its target genes, increased expression of certain miRNAs is expected to be associated with a decrease in the level of its target gene(s). Hence, we performed Gene array assay using mRNA prepared from SH-SY5Y cells untreated or treated with 10 pg/ml of Vpr protein for 24 h. We then investigated the levels of several selected genes involved in neuronal regulation and also known to be miR-1, miR-7, miR-34a/b, or miR-96 targets Interestingly, Gene array assay showed that the levels of the selected genes decreased by at least 2-fold while the levels of their associated miRNAs increased in Vpr-treated cells compared with the mock untreated (Table 1). Functions of the genes are listed (right column). These results further supporting the hypothesis that Vpr is involved in neuronal deregulation. Similar results were obtained with HN cells treated with Vpr (data not shown).

Validation of Target Genes Expression by qPCR—Next, we sought to validate our data using SH-SY5 cells (5×10^5) were treated with 10 pg/ml of Vpr protein for 24 h. Total RNA was prepared from one set (set 1) and processed for quantitative PCR while protein extracts were prepared from the second set (set 2) and used for Western blot analysis.

The status of five selected target genes (IRBIT, SERP1, NEFM, Drp1 and CREB) that are known to be targeted by miRs-1, -7, -34a, and -96 was examined. These genes are known to be involved in neuronal regulation. For example, dephosphorylation and inhibition of the IP_3R-binding protein (IRBIT) released with IP_3 leads to Ca^{2+} release from the ER and causes aberrant neuronal regulation (32), while the stress-associated endoplasmic reticulum protein 1 (SERP1) has been shown to stabilize ER membrane proteins during stress (33) and protects unfolded target proteins against degradation during ER stress. Similarly, maintaining the proper axon diameter size is essential for the conduction of nerve impulses (34). Further, distribution of the mitochondria inside the axon is essential to control ATP levels and cell-to-cell communication. The neurofilament medium polypeptide (NEFM) (35) protein and the Dynamin-related Protein (Drp-1) (36) are the main proteins involved in these events. Finally, ER stress activates CREB through TOX3 while CREB is a target gene of miR-34a and involved in neurites growth and synaptic plasticity (14).

As shown in Fig. 4, the RNA and protein levels of IRBIT, SERP1, NEFM, Drp-1 and CREB decreased, as measured by qPCR (*panel A*) and Western blot (*panel B*), respectively, in Vpr-treated cells when compared with the controls untreated. These results point to the ability of Vpr to cause ER stress, to promote ER Ca^{2+} release, and to affect mitochondrial distribution. Differences in the levels of expression of these proteins were further evaluated by densitometry analysis using EZQuant-Gel software Software. As shown in *panel C*, the proteins levels decreased in Vpr-treated cells compared with untreated cells.

To further validate our observations, we performed an immunohistochemistry assay using brain tissues prepared from control parental or Vpr-transgenic mice (7). As shown in Fig. 4*D*, Vpr reduces the levels of CREB protein (rhodamine) and promotes its translocation to the nucleus of the cells when compared with the control. MAP-2 (fluorescein) was used to dem-

A.

miRs Up-regulated in Vpr-treated SH-SY5Y (>2 fold)		
miR-1	miR-196a	miR-449a
miR-7	miR-199a-3p	miR-496
miR-7-1	miR-200a	miR-507
miR-34a, b	miR-302b	miR-512-3p
miR-96	miR-302c	miR-515-3p
miR-134	miR-371-3p	miR-518a
miR-146a	miR-373	miR-520b
miR-147	miR-378	miR-520e
miR-148a	miR-383	miR-592
miR-182	miR-429	miR-603
miRs Down-regulated in Vpr-treated SH-SY5Y (<2 fold)		
miR-29a	miR-133b	miR-421
miR-106b	miR-139-5p	miR-488
miR-122	miR-325	miR-510
miR-125b	miR-335	miR-566
miR-132	miR-361	miR-612

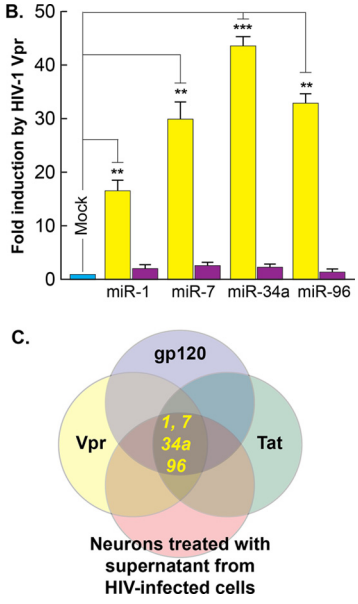

FIGURE 3. **miRNAs levels in Vpr-treated cells.** *A*, list of the miRNAs that are differentially expressed ($> 2 <$ fold) in Vpr-treated SH-SY5Y cells. *B*, fold changes of 4 selected miRNAs in Vpr-treated cells compared with the control obtained by qPCR. The experiment was repeated three times, the results are statistically significant using Student's *t* test ($p < 0.05$ is indicated by ** compared with the mock control group [one-way analysis of variance and ANOVA Test]). *C*, Venn diagram of the overlap of the most differentiated miRNAs in cells treated with Vpr, Tat, gp120 proteins, or with supernatant from HIV-1-infected U-937 cells. The miRNAs differentially expressed are depicted in the overlapping area of the *four circles*.

TABLE 1

Status of selected target genes in Vpr-treated cells

SH-SY5Y cells were treated with 10 pg/ml of Vpr for 24 hours, after which the RNA was isolated and subjected to gene array assay (Only selected affected genes and their associated miRNAs are shown).

miRs	Genes	Functions
miR-1	SERP1 (Stress-associated endoplasmic reticulum protein 1)	Stabilizes ER membrane during stress
miR-7	NEFM (Neurofilament medium polypeptide)	Nerve functions and maintaining axonal diameter
miR-34a/b	Drp-1 (Dynamin-related protein)	Mitochondrial distribution inside the axon & divisior
	CACNB1 (Voltage-dependent l-type Ca^{2+} channel subunit β-1)	Controls Ca^{2+} release
	SIRT-1 (Sirtuin)	Synaptic plasticity and neurons protection
	STIM1 (Stromal interaction molecule 1)	Control Ca^{2+} Influx
	CREB (cAMP response element-binding)	Transcription factor
miR-96	IRBIT (IP(3)R-binding protein released with IP(3))	Control Ca^{2+} release from the ER

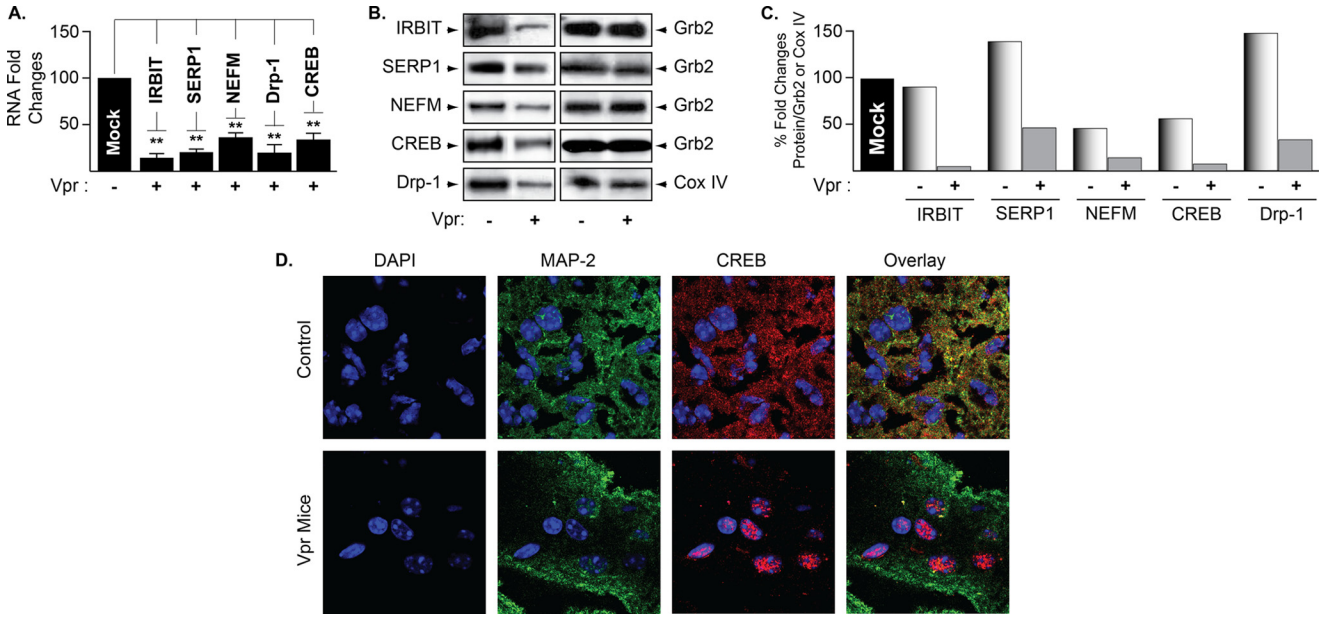

FIGURE 4. **miRNAs and their target genes levels in Vpr-treated cells.** *A* and *B*, qPCR and Western blot analysis point to the ability of Vpr to decrease the RNA and proteins levels of IRBIT, SERP1, NEFM, Drp-1, or CREB. Anti-IRBIT, -SERP1, -NEFM, -Drp1, -CREB, -Grb-2, or -Cox IV antibodies were used as indicated. Fold changes are displayed as histograms. The experiment (qPCR) was repeated three times, and the results were analyzed by Student's *t* test statistical significance level, $p < 0.05$ is indicated by ** compared with the mock control group (one-way analysis of variance and ANOVA test). *C*, histogram represents the variations in the target genes levels obtained by Western assays and measured relatively to Grb2 or cox IV (for Drp-1) using densitometric analysis (EZQuant-Gel software); the control (Mock) was set arbitrarily at 100%. *D*, distribution of CREB protein (*red*) in the brain of Vpr-transgenic mice compared with the control mice. MAP-2 (*green*) and DAPI (*blue*) staining were used as a control.

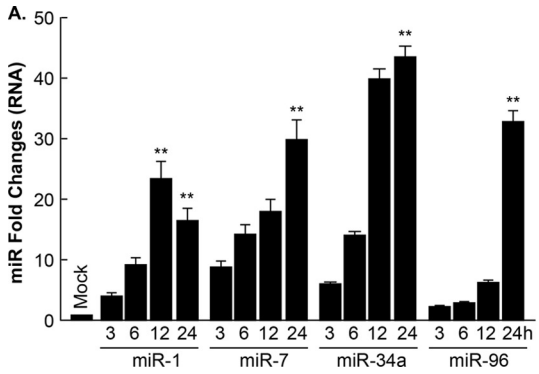

B.

Gene	3h	6h	12h	24h
IRBIT	0.823	0.763	0.311	0.442
SERP1	0.734	0.669	0.621	0.419
Orai	1.230	0.981	0.541	0.372
STIM1	1.102	0.543	0.737	0.301
IP3R	1.098	0.872	0.649	0.485
CREB	0.872	0.611	0.652	0.541
Drp-1	0.711	0.658	0.561	0.440
NEFM	0.884	0.801	0.772	0.475
SIRT1	0.861	0.671	0.630	0.501

RNA Fold Changes

FIGURE 5. **Vpr deregulation of miRNAs and genes is time-dependent.** RNA fold changes of selected miRNAs (*A*) or genes (*B*) in Vpr-treated SH-SY5Y cells using time point (3, 6, 12, and 24 h) compared with control (*Mock*) obtained by qPCR. Each experiment was repeated three times, the results were analyzed by Student's *t* test statistical significance level, $p < 0.05$ is indicated by ** compared with the mock control group (one way analysis of variance and ANOVA test).

onstrate the neuronal nature of the cells and DAPI (blue) was used to highlight the nuclei.

Is the Effect of Vpr Time-dependent?—It is well known that miRNAs can be deregulated as soon as a stimulus is introduced. Thus, we examined whether deregulation of the miRNAs and their target genes is time-dependent. SH-SY5Y cells were treated with 10 pg/ml of Vpr protein for 3, 6, 12, and 24 h. RNA was prepared, the levels of the 4 selected miRNAs (Fig. 5*A*) and their target genes (*panel B*) were measured by qPCR. Vpr increases the levels of miRNAs as early as 3 h to reach a peak at 24 h before start declining (data not shown). miR-1 presents an exception where the highest increase was observed at 12 h. The levels of the target genes start decreasing as of 3 h to reach a peak at 24 h (*panel B*).

The Effect of Vpr is miRNA-dependent—Induction of the specific miRNAs by Vpr and inhibition of their target genes prompted us to examine the status of the target genes in the absence of their associated miRNAs. SH-SY5Y cells were transfected with anti-miR-34a for 24 h, then treated with 10 pg/ml of Vpr protein. Total RNA was isolated and the levels of selected genes that are regulated by miR-34a were examined by qPCR. As shown in Fig. 6*A*, Vpr decreased the mRNA levels of these genes (red) in the presence of miR-34a but not in its absence (yellow). Interestingly, the RNA levels of these genes did increase in cells transfected with anti-miR-34a (green), which corroborate with previous data regarding the ability of anti-miR34a to rescue the cells from apoptosis and to up-regulates miR-34a target genes (37). These results placed miR-34a as a major player involved in neuronal deregulation induced by Vpr.

To further confirm this hypothesis, we performed *in situ* hybridization (ISH) assay to examine the status of miR-34a *in vivo* in the brain of Vpr transgenic mice. ISH of brain tissues prepared from control or Vpr-transgenic mice showed that Vpr

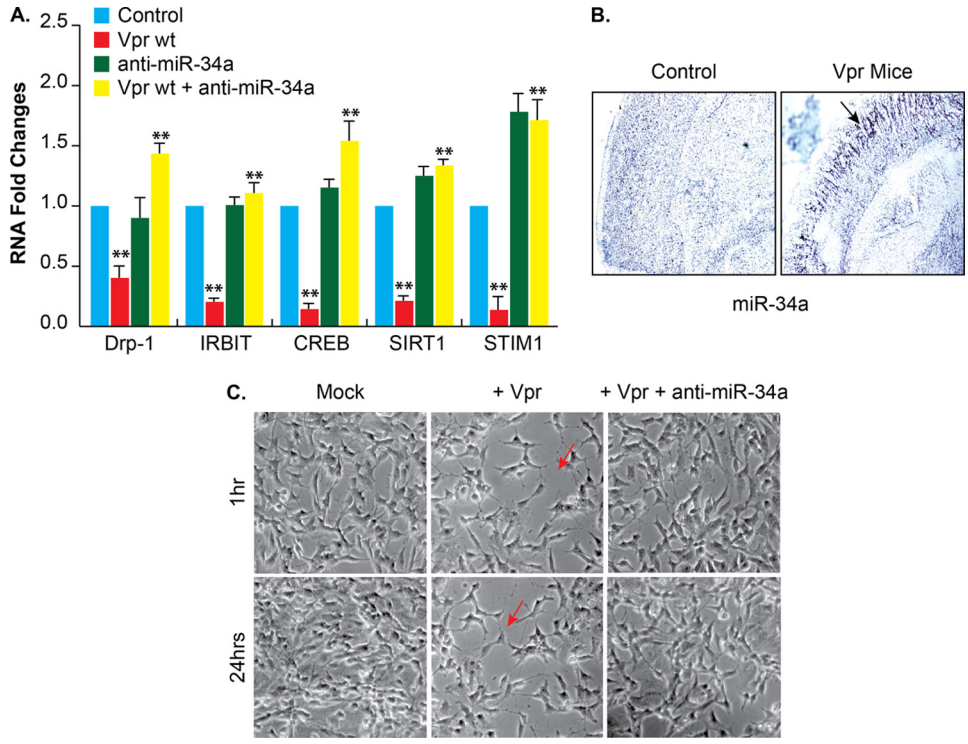

FIGURE 6. **Vpr failed to affect selected genes in the presence of anti-miR-34a.** *A*, qPCR results point to the ability of Vpr to decrease the RNA levels of Drp-1, IRBIT, SERP1, CREB, SIRT1, and STIM1 in the absence of anti-miR-34a (*red*) but not in its presence (*yellow*) as indicated. Fold changes are displayed as histograms. The experiments were repeated three times, and the results were analyzed by Student's *t* test statistical significance level, $p < 0.05$ is indicated by ** compared with the mock control group. *B*, distribution of miR-34a in the brain of Vpr-transgenic mice (*arrow*) compared with the control mice. miR-34a localizes more to the cortical region in these mice. *C*, neuronal processes were affected by Vpr and restored in the presence of anti-miR-34a.

increases the levels of miR-34a *in vivo* when compared with the control parental mice (*panel B*, *arrow*).

In parallel, we examined whether inhibition of miR-34a restores neurites length and thus neuronal communication especially since miR-34a target genes: SIRT1 and CREB are involved in this phenomenon. Addition of Vpr protein to SH-SY5Y cells causes neurites retraction and only 20–30% of cell death when compared with the mock-untreated cells. Interestingly, Vpr protein failed to affect the neurite lengths in the presence of anti-miR-34a (*panel C*).

Validation of the Data in HN Cells—Because Vpr is not the only HIV-1 secreted protein, we decided to examine its effect on the four selected miRNAs and their target genes when secreted from HIV-1 infected cells. We also sought to validate our data using primary human cultures (HN) treated with recombinant Vpr protein. To that end, SH-SY5Y cells were treated with supernatant prepared from HIV-1-infected U-937 cells while HN cells were treated with 10 pg/ml of Vpr protein. Twenty-four hours later, RNA was isolated and used for qPCR assay. As expected, an increase in the levels of the four selected miRNAs and a decrease in the levels of the target genes were observed in both cell types when compared with the mock (Table 2). The mock (untreated cells) and GAPDH were set at 1. These results confirm the ability of recombinant and/or secreted Vpr proteins to promote neuronal deregulation. These results also proved that SH-SY5Y cell line is a good model to be used in future studies.

TABLE 2

Effect of Vpr on selected genes in HN and *in vivo*

qPCR results point to the ability of Vpr protein (recombinant or secreted) or the supernatant from infected cells to increase the levels of the selected miRNAs in HN and SH-SY5Y cells. Vpr also decreases the RNA levels of several target genes in the same samples as indicated. The experiment was repeated three times. The results are statistically significant using Student's *t* test ($p < 0.05$ compared with the mock control group (one-way analysis of variance & ANOVA test)).

miRNA	HN cells	SH-SY5Y treated with sup from HIV
miR-1	12.35 ± 3.87	11.34 ± 4.01
miR-7	14.96 ± 3.60	15.53 ± 4.88
miR-34a	43.56 ± 9.08	28.62 ± 6.27
miR-96	31.82 ± 11.24	19.56 ± 5.42
Gene	**HN cells**	**SH-SY5Y treated with Sup from HIV**
IRBIT	0.478 ± 0.031	0.328 ± 0.015
SERP1	0.313 ± 0.029	0.435 ± 0.026
NEFM	0.603 ± 0.048	0.612 ± 0.031
CREB	0.344 ± 0.025	0.321 ± 0.037
Drp-1	0.557 ± 0.030	0.358 ± 0.043
STIM1	0.166 ± 0.009	0.310 ± 0.027
SIRT1	0.626 ± 0.053	0.538 ± 0.049
IP3R	0.555 ± 0.035	0.479 ± 0.042

DISCUSSION

In this study, we demonstrated the ability of HIV-1 Vpr to cause neuronal deregulation through a pathway that is miRNAs-dependent. First, we identify the miRNAs and their target genes affected by the presence of Vpr in human neurons (primary cultures and cell line) and later we validated the levels of these miRs and genes by qPCR, Western blot and immunostaining assays.

Previous studies demonstrated the ability of Vpr and/or miRNAs to cause neuronal deregulation, separately. However,

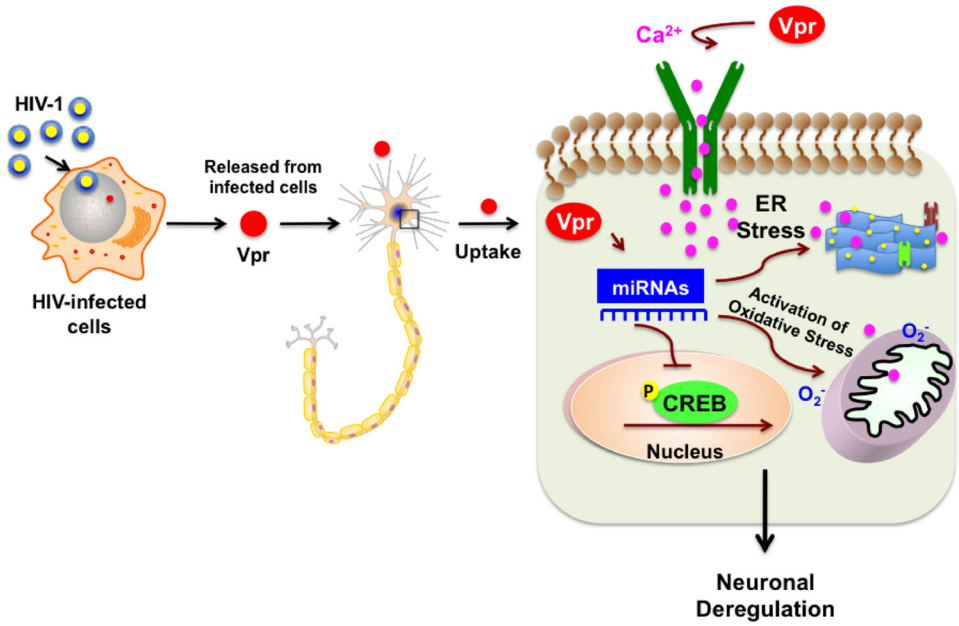

FIGURE 7. **Schematic representation of the proposed pathways used by Vpr to promote neuronal degeneration.** Vpr could disturb calcium balance by affecting L- or P/Q-type calcium channels through a signaling pathway, yet to be identified that could lead to miRNAs deregulation and eventually neuronal dysfunction. Vpr can also be taken up by neurons and can affect miRNAs level directly which leads to neuronal dysfunction. Our results point to the ability to induce both pathways.

TABLE 3

Deregulated genes involved in calcium homeostasis in Vpr-treated SH-SY5Y cells

The table represents some of the cellular genes that are differentially expressed in Vpr-treated neurons and involved in calcium regulation.

Genes	Name	Function
GRIN1	Glutamate [NMDA] receptor subunit zeta-1	Ca^{2+} ion homeostasis
HRC	Sarcoplasmic reticulum histidine-rich Ca^{2+}-binding protein	Ca^{2+} ion homeostasis
ATP2A1	Sarcoplasmic/endoplasmic reticulum calcium ATPase 1	Calcium ion import
CACNA1A	Voltage-dependent P/Q-type Ca^{2+} channel subunit α-1A	Calcium ion transport
CACNA1F	Voltage-dependent l-type calcium channel subunit α-1F	Calcium ion transport
CACNA1S	Voltage-dependent l-type calcium channel subunit α-1S	Calcium ion transport
CACNB1	Voltage-dependent l-type calcium channel subunit β-1	Calcium ion transport
GRIN3A	Glutamate [NMDA] receptor subunit 3A	Calcium ion transport
STIM1	Stromal interaction molecule 1	Calcium ion transport
STIM2	Stromal interaction molecule 2	Calcium ion transport
TPCN2	Two pore calcium channel protein 2	Calcium ion transport

the exact relation between Vpr-miRNAs and neuronal dysfunction was not investigated. To that end, we sought to decipher this relation and examine whether this interplay is involved in the development of HAND. The ability of Vpr to cause neuronal deregulation was examined by several laboratories including ours, however the molecular mechanisms involved were unclear. Vpr was shown to disturb neuronal Ca^{2+} homeostasis through down-regulation of endogenous PMCA (13), to inhibit axonal growth through induction of mitochondrial dysfunction (10) and to induce apoptosis in CNS cells *in vitro* and *in vivo* (38). Vpr was shown to perform these functions through a domain that encompasses amino acids 70 to 96 (C-terminal domain) (39). The expression of Vpr in the neurons of HIV-1 infected patients with encephalitis (HIVE) was also described (7). However, these published studies lack mechanistic explanations for the observed phenomena.

Similarly, small RNA in general and miRNAs in particular has been described to be involved in neuronal deregulation and in the development of neurodegenerative diseases. In this regard, miRNAs have been shown to be involved in psychiatric disorders (40) such as schizophrenia and bipolar disorders (41). Further, the link between miRNAs and neurodegenerative diseases such as Alzheimer disease, Huntington disease, and Parkinson disease is becoming increasingly evident (42, 43). miRNAs were also shown to be involved in the pathogenesis of neuroblastoma and astrocytoma (44, 45).

Strikingly, miR-34a is among the miRNAs involved in these events. Identified by Welch *et al.* (46), miR-34a was shown to be involved in cell cycle progression, cellular senescence and apoptosis; however its targets (in addition to the ones described in this study) remain to be defined. Among miR-34a targets, p53 and SIRT1 were the most studied and shown to be involved in apoptosis or cell survival (47). miR-34a was recently shown to behave like a tumor suppressor in brain tumors and glioma stem cells (48). In addition to its involvement in tumors, miR-34a was also shown to play a role in neurodegenerative diseases and psychiatric problems. In fact, miR-34a was demonstrated as one of the miRNAs involved in mood disorders (40), schizophrenia and bipolar disorders (41), and Alzheimer disease (49). miR-34a was also shown to be functionally linked to Bcl-2 down-regulation. miR-34a was suggested to down-regulate the Bcl-2

promoter by preventing the phosphorylation of CREB (14), which corroborate our data.

Interestingly, while we demonstrated that the level of miR-34a increases in Vpr-treated neurons and in neurons treated with supernatant prepared from HIV-1-infected U-937 cells, this level decreases in PBMC isolated from HIV-1-infected patients (50). The difference is mainly due to the fact that PBMC, and not neurons, can be infected with HIV-1. This observation further establishes the relation between the miRNAs (mainly miR-34a), Vpr, and neuronal regulation. Furthermore, the ability of Vpr to indirectly inhibit miR-34a target genes and renders them inactive, led us to conclude that Vpr is using this mechanistic pathway to cause neuronal deregulation, neuronal loss, and eventually the development of HIV-1-associated cognitive disorders (HAND). We also demonstrated that such a phenomenon could be prevented in the presence of anti-miR-34a. These results confirm our hypothesis regarding involvement of miRNAs in neurodegenrative diseases and lead to the conclusion that the next challenge is to translate these data into therapeutic intervention to prevent the development of HAND.

Alternatively, our results raised a challenging question regarding the ability of HIV-1 proteins (*e.g.* Vpr) to play a role in neuronal deregulation in the HAART era. The answer to this highly challenging question and the pathways involved in the development of HAND, besides the one studied here, remain unclear. Nevertheless, there are compelling neuropathological data showing that the HAND disease process occurs with the ongoing presence of virus and despite the therapy, HAND remains very prevalent (51–53). On the other hand, in a recent study, it was described that HIV-1 infects multipotent hematopoietic stem and progenitor cells. These cells allow the virus to hide and to be reactivated and re-infect additional cells even in the HAART era (54). Although the reasons for the reactivation of latent viruses are unclear, the Siliciano group describes that deregulation of miRNAs could lead to latent HIV-reactivation (53). As a result, it is expected that viral proteins released by latent reactivated viruses continue to play a role along with miRNAs in the development of HAND.

In summary, though we demonstrate that Vpr is able to affect neuronal dysfunction by altering miRNA expressions, the pathway used by Vpr needs to be further evaluated. It may be that the increased expression of miR-34a may simply be the result of the Ca^{2+} mobilization since that mobilization mediates numerous signaling pathways (Fig. 7). To clarify this hypothesis, we examined the target genes involved in calcium homeostasis and deregulated in neurons in the presence of Vpr. As shown in Table 3, gene array data point to the ability of Vpr to affect the expression levels (positively or negatively) of several genes involved in calcium homeostasis, further demonstrating the role Vpr plays in altering the cell's calcium homeostasis/mobilization. These results led us to suggest the presence of a tight link between Vpr-calcium release and the development of HAND (Fig. 7). However, considering that several studies have shown how Vpr can also affect signal transduction pathways, elucidating the exact pathway that soluble Vpr hijacks in neurons may prove useful in understanding HAND and may provide novel therapeutic targets.

Acknowledgments—The content is solely the responsibility of the authors and does not necessarily represent the official views of Harvard Catalyst, Harvard University, and its affiliated academic health care centers, the National Center for Research Resources, or the National Institutes of Health.

REFERENCES

1. Kaul, M. (2008) *Front. Biosci.* **13,** 2484–2494
2. Aquaro, S., Svicher, V., Ronga, L., Perno, C. F., and Pollicita, M. (2008) *Recent Patents CNS Drug Discov.* **3,** 23–33
3. González-Scarano, F., and Martín-García, J. (2005) *Nat. Rev. Immunol.* **5,** 69–81
4. Poluektova, L., Meyer, V., Walters, L., Paez, X., and Gendelman, H. E. (2005) *Glia* **52,** 344–353
5. Kaul, M., and Lipton, S. A. (2006) *Curr. HIV Res.* **4,** 307–318
6. Anthony, I. C., and Bell, J. E. (2008) *Int. Rev. Psychiatry* **20,** 15–24
7. Jones, G. J., Barsby, N. L., Cohen, E. A., Holden, J., Harris, K., Dickie, P., Jhamandas, J., and Power, C. (2007) *J. Neurosci.* **27,** 3703–3711
8. Pandey, R. C., Datta, D., Mukerjee, R., Srinivasan, A., Mahalingam, S., and Sawaya, B. E. (2009) *Curr. HIV Res.* **7,** 114–128
9. Nitahara-Kasahara, Y., Kamata, M., Yamamoto, T., Zhang, X., Miyamoto, Y., Muneta, K., Iijima, S., Yoneda, Y., Tsunetsugu-Yokota, Y., and Aida, Y. (2007) *J. Virol.* **81,** 5284–5293
10. Kitayama, H., Miura, Y., Ando, Y., Hoshino, S., Ishizaka, Y., and Koyanagi, Y. (2008) *J. Virol.* **82,** 2528–2542
11. Jacquot, G., Le, Rouzic, E., David, A., Mazzolini, J., Bouchet, J., Bouaziz, S., Niedergang, F., Pancino, G., and Benichou, S. (2007) *Retrovirology* **4,** 84
12. Zhao, R. Y., Elder, R. T., and Bukrinsky, M. (2007) *Adv. Pharmacol.* **55,** 233–260
13. Rom, I., Deshmane, S. L., Mukerjee, R., Khalili, K., Amini, S., and Sawaya, B. E. (2009) *Brain Res.* **1275,** 81–86
14. Zieg, J., Greer, P. L., and Greenberg, M. E. (2008) *Cell* **134,** 1080–1080.e2
15. Yamakage, M., and Namiki, A. (2002) *Can. J. Anaesth.* **49,** 151–164
16. Fill, M., and Copello, J. A. (2002) *Physiol. Rev.* **82,** 893–922
17. Mattson, M. P., and Chan, S. L. (2003) *Nat. Cell Biol.* **5,** 1041–1043
18. Boehning, D., van Rossum, D. B., Patterson, R. L., and Snyder, S. H. (2005) *Proc. Natl. Acad. Sci. U.S.A.* **102,** 1466–1471
19. Sun, F., and Cavalli, V. (2010) *Mol. Cell. Proteomics.* **9,** 963–975
20. Hollenbeck, P. J., and Saxton, W. M. (2005) *J. Cell Sci.* **118,** 5411–5419
21. Sonntag, K. C. (2010) *Brain Res.* **1338,** 48–57
22. Eacker, S. M., Dawson, T. M., and Dawson, V. L. (2009) *Nat. Rev. Neurosci.* **10,** 837–841
23. Barbato, C., Ruberti, F., and Cogoni, C. (2009) *J. Biomed. Biotechnol.* **87,** 1313
24. Rossbach, M. (2010) *Curr. Mol. Med.* **10,** 361–368
25. Singh, S. K. (2007) *Pharmacogenomics* **8,** 971–978
26. Das, A. T., Brummelkamp, T. R., Westerhout, E. M., Vink, M., Madiredjo, M., Bernards, R., and Berkhout, B. (2004) *J. Virol.* **78,** 2601–2605
27. Brailoiu, G. C., Oprea, T. I., Zhao, P., Abood, M. E., and Brailoiu, E. (2011) *J. Biol. Chem.* **286,** 29166–29174
28. Sawaya, B. E., Khalili, K., Mercer, W. E., Denisova, L., and Amini, S. (1998) *J. Biol. Chem.* **273,** 20052–20057
29. Dickie, P., Roberts, A., Uwiera, R., Witmer, J., Sharma, K., and Kopp, J. B. (2004) *Virology* **322**, 69–81
30. Wheeler, E. D., Achim, C. L., and Ayyavoo, V. (2006) *J. Neurovirol.* **12,** 200–210
31. Henklein, P., Bruns, K., Sherman, M. P., Tessmer, U., Licha, K., Kopp, J., de, Noronha, C. M., Greene, W. C., Wray, V., and Schubert, U. (2000) J. *Biol. Chem.* **275,** 32016–32026
32. Ando, H., Mizutani, A., Kiefer, H., Tsuzurugi, D., Michikawa, T., and Mikoshiba, K. (2006) *Mol. Cell* **22,** 795–806
33. Yamaguchi, A., Hori, O., Stern, D. M., Hartmann, E., Ogawa, S., and Tohyama, M. (1999) *J. Cell Biol.* **147,** 1195–1204
34. Ellis, R., Langford, D., and Masliah, E. (2007) *Nat. Rev. Neurosci.* **8,** 33–44
35. Kriz, J., Zhu, Q., Julien, J. P., and Padjen, A. L. (2000) *Brain Res.* **885,** 32–44
36. Smirnova, E., Shurland, D. L., Ryazantsev, S. N., and van der Bliek, A. M.

(1998) *J. Cell Biol.* **143,** 351–358
37. Roggli, E., Britan, A., Gattesco, S., Lin-Marq, N., Abderrahmani, A., Meda, P., and Regazzi, R. (2010) *Diabetes.* **59,** 978–986
38. Cheng, X., Mukhtar, M., Acheampong, E. A., Srinivasan, A., Rafi, M., Pomerantz, R. J., and Parveen, Z. (2007) *DNA Cell Biol.* **2,** 116–131
39. Sabbah, E. N., and Roques, B. P. (2005) *J. Neurovirol.* **11,** 489–502
40. Zhou, R., Yuan, P., Wang, Y., Hunsberger, J. G., Elkahloun, A., Wei, Y., Damschroder-Williams, P., Du, J., Chen, G., and Manji, H. K. (2009) *Neuropsychopharmacology* **34,** 1395–1405
41. Kim, A. H., Reimers, M., Maher, B., Williamson, V., McMichael, O., McClay, J. L., van den Oord, E. J., Riley, B. P., Kendler, K. S., and Vladimirov, V. I. (2010) *Schizophrenia Res.* **124,** 183–191
42. Laua, P., and Bart de Stroopera, B. (2010) *Sem. Cell Dev. Biol.* **21,** 768–773
43. Bushati, N., and Cohen, S. M. (2008) *Curr. Opin. Neurobiol.* **18,** 292–296
44. Stallings, R. L. (2009) *Curr. Pharm. Des.* **15,** 456–462
45. Moser, J. J., and Fritzler, M. J. (2010) *PLoS One* **5,** e13445
46. Welch, C., Chen, Y., and Stallings, R. L. (2007) *Oncogene* **26,** 5017–5022
47. Yamakuchi, M., and Lowenstein, C. J. (2009) *Cell Cycle* **8,** 712–715
48. Guessous, F., Zhang, Y., Kofman, A., Catania, A., Li, Y., Schiff, D., Purow, B., and Abounader, R. (2010) *Cell Cycle* **9,** 1031–1036
49. Schipper, H. M., Maes, O. C., Chertkow, H. M., and Wang, E. (2007) *Gene Reg. Sys. Biol.* **1,** 263–274
50. Houzet, L., Yeung, M. L., de, Lame, V., Desai, D., Smith, S. M., and Jeang, K. T. (2008) *Retrovirology* **5,** 118
51. Vivithanaporn, P., Heo, G., Gamble, J., Krentz, H. B., Hoke, A., Gill, M. J., and Power, C. (2010) *Neurology* **75,** 1150–1158
52. Everall, I., Vaida, F., Khanlou, N., Lazzaretto, D., Achim, C., Letendre, S., Moore, D., Ellis, R., Cherner, M., Gelman, B., Morgello, S., Singer, E., Grant, I., and Masliah, E. (2009) *J. Neurovirol.* **15,** 360–370
53. Han, Y., and Siliciano, R. F. (2007) *Nat. Med.* **3,** 1138–1140
54. Carter, C. C., McNamara, L. A., Onafuwa-Nuga, A., Shackleton, M., Riddell, J., 4th, Bixby, D., Savona, M. R., Morrison, S. J., and Collins, K. L. (2011) *Cell Host Microbe* **9,** 223–234